

CHAPTER -10

RELAXATION PHENOMENA OF APROTIC POLAR LIQUID MOLECULES UNDER A KILOHERTZ ELECTRIC FIELD

RELAXATION PHENOMENA OF APROTIC POLAR LIQUID MOLECULES UNDER A KILOHERTZ ELECTRIC FIELD

10.1. Introduction

The experimental determination of radio frequency (rf) conductivity σ'_{ij} of polar-nonpolar liquid mixture is of special interest as it provides an information of various relaxation parameters like free ion density 'n', relaxation time τ_j , dipole moment μ_j and thermodynamic energy parameters including the activation energy ΔE_j of a polar solute. These measured parameters helps one to ascertain shape, size and structure of a polar molecule, in addition to solute-solvent (monomer) and solute-solute (dimer) molecular associations.

According to Murphy and Morgan [1] displacement current is the only factor to yield electrical conduction in a pure polar dielectric liquid. But for almost all the insulating dipolar liquids electrical conduction arises due to the combined effects of displacement current and ohmic current arising out of actual charge transfer [2-4]. In microwave (mw) electric field the mobility of free charge carriers ceases, but in rf electric field below 20 MHz the dielectric loss ϵ'' for the free charge transfer in dielectropolar liquids gives a significant contribution to rf conductivity σ'_{ij} . Cosmic rays, natural radioactivity, thermal dissociation etc. are supposed to be the main sources of the presence of free ions and electrons in liquid dielectrics. But no concrete conclusion have not yet been reached so far regarding such ion formation in a dipolar liquid.

Sen and Ghosh [5,6] took into account of such type of electrical conduction in rf electric field and showed that σ'_{ij} is a linear function of reciprocal of solution viscosity η_{ij} . We applied this formulation on two aprotic polar liquids : N, N dimethyl formamide (DMF) and dimethyl sulphoxide (DMSO) in both C_6H_6 and CCl_4 in the temperature range of 30°C to 60°C under 500KHz electric field. The slope of the linear relation between σ'_{ij} and $1/\eta_{ij}$

(Eq 10.1) as shown by the straight line curves of Figure 10.1 is used to estimate free ion density 'n' in terms of molecular radius 'a' obtained from gas kinetic theory. The estimated slope and hence n are placed in Table 10.2. Einstein-Stokes relation [7] is further employed to get τ_j at different concentrations w_j 's and at different temperatures as seen in Table 10.1. τ_j at infinite dilution is, however, obtained from $\tau_j - w_j$ fitted equations to get dipole moment under rf electric field at different temperatures by Smyths' relation [8] in terms of linear coefficient β of $\sigma'_{ij} - w_j$ fitted curves, in order to place them in Table 10.2. The theoretical dipole moment μ_{theo} obtained from available bond angles and bond moments of flexible polar groups attached to parent molecule as seen elsewhere [9] are then compared with these measured μ_j 's. The comparison, however, showed that the structural conformations of such liquids are correct. The variation of μ_j with temperature in $^{\circ}\text{C}$ as seen in Figure 10.2 further provides a valuable information regarding molecular association.

It is evident from Figure 10.3 that $\ln \sigma'_{ij}$ displays a linear relationship with $1/T$, where T is temperature in Kelvin. The slope of the least squares fitted straight line curves of Figure 10.3 has conveniently been used to estimate the semiconduction activation energy ΔE_j at different concentrations. The measured ΔE_j are entered in the 7th column of Table 10.3. The variation of τ_j with temperature prompted us to obtain thermodynamic energy parameters ΔH_{τ} , ΔS_{τ} and ΔF_{τ} from Eyrings rate theory [10]. The dimensionless parameter $\gamma (= \Delta H_{\tau} / \Delta H_{\eta})$ was estimated from linear relationship between $\ln \tau_j T$ and $\ln \eta$. γ was used to get the energy of activation ΔH_{η} due to viscous flow. It finally indicates the solvent environment around solute molecules [11]. The estimated energy parameters along with γ are entered in Table 10.4 to conclude about either stability or unstability [9, 11, 12] of polar-nonpolar liquid mixtures under rf electric field. The Debye and Kalman factors $\tau_j T / \eta$ and $\tau_j T / \eta^{\gamma}$, as seen in the 8th and 9th columns of Table 10.3 were computed to suggest that measured data of such aprotic polar liquids obey Debye relaxation behaviour.

The purpose of the present paper is to test the adequacy or otherwise of the theoretical formulation so far derived [5,6] and the modified formulations presented in the chapter 2 of this thesis. A clear concept about structural conformation and molecular associations of the said polar liquids could, however, be attained. In addition this paper also provides an experimental verification of the results obtained in case of DMF + DMSO in C_6H_6 under GHz electric field of chapter 3 of this thesis. Although dielectric relaxation studies have been carried out on several dipolar liquids under rf electric field by many workers [13-16], but rf σ'_{ij} measurement for such aprotic polar liquids have not yet been made.

10.2. Rf Experimental details

The block diagram of the experimental set up and the theoretical formulation to estimate σ'_{ij} and other physical parameters of a polar-nonpolar (ij) liquid mixture have been presented in detail in chapter 2. A cylindrical glass tube made up of pyrex glass of diameter 2 cm is used as a dielectric cell which is fitted with a pair of stainless steel electrodes of diameter 1.5 cm and separated by 1cm. The Analar grade N, N dimethyl formamide (DMF), dimethyl sulphoxide (DMSO), benzene C_6H_6 , carbon tetrachloride CCl_4 were obtained from E. Merck (Germany). They were distilled in vacuum and kept in a dessicator before use. The viscosity of the experimental liquids were measured at different temperatures by an Ostwald viscometer with highly pure distilled water as a reference fluid. The temperature of all the experiments were controlled by a highly sensitive thermostat whose accuracy was $\pm 0.5^\circ C$. Other physical constants like density ρ , static relative permittivity ϵ_0 and refractive index n_D were carefully checked in agreement with literature values [17].

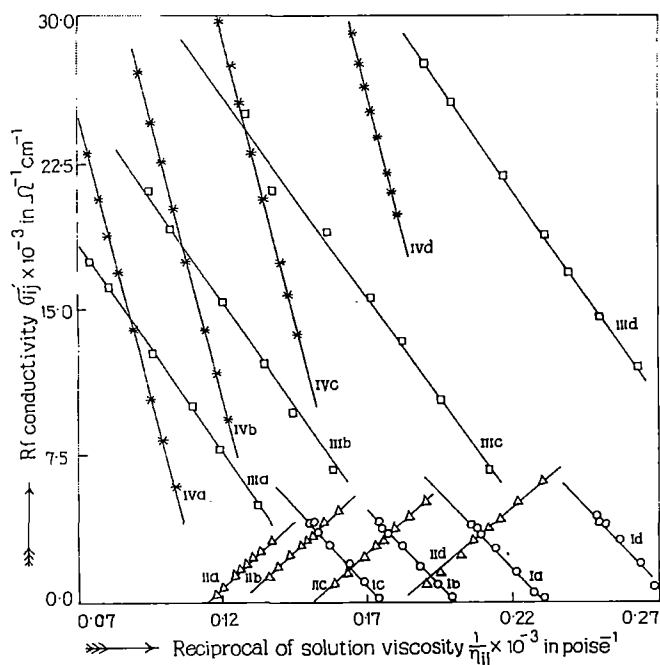


Figure 10.1: Linear variation of rf conductivity σ'_{ij} against reciprocal of solution viscosity $1/\eta_{ij}$ of aprotic polar liquids in benzene and carbon tetrachloride at different experimental temperatures under 500 KHz electric field.

(I) DMF in C_6H_6 (—○—), (Ia) at 30°C, (Ib) at 40°C, (Ic) at 50°C, (Id) at 60°C.

(II) DMF in CCl_4 (—△—), (IIa) at 30°C, (IIb) at 40°C, (IIc) at 50°C, (IIb) at 60°C.

(III) DMSO in C_6H_6 (—□—), (IIIa) at 30°C, (IIIb) at 40°C (IIIc) at 50°C, (IIId) at 60°C.

(IV) DMSO in CCl_4 (—*—), (IVa) at 30°C, (IVb) at 40°C, (IVc) at 50°C, (IVd) at 60°C.

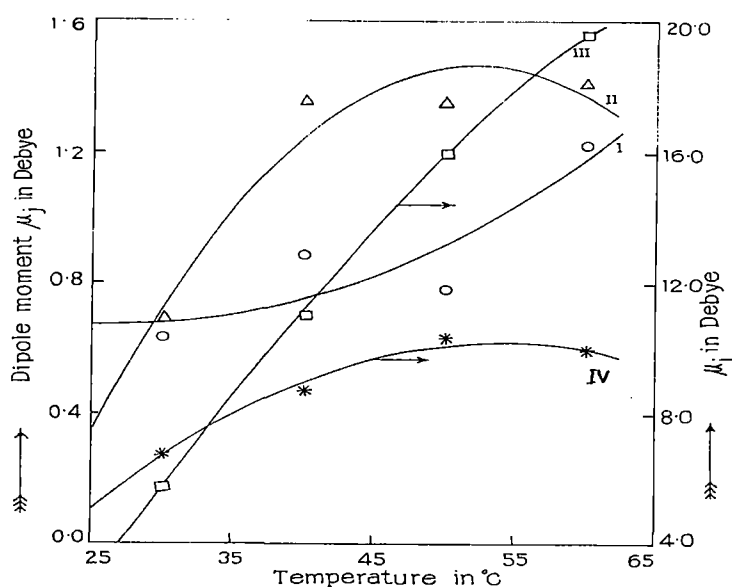


Figure 10.2: Plot of dipole moment μ_j in Debye against temperature in °C of aprotic polar liquids in C_6H_6 and CCl_4 under 500KHz electric field.

(I) DMF in C_6H_6 (—○—), (II) DMF in CCl_4 (—△—), (III) DMSO in C_6H_6 (—□—),

(IV) DMSO in CCl_4 (—*—)

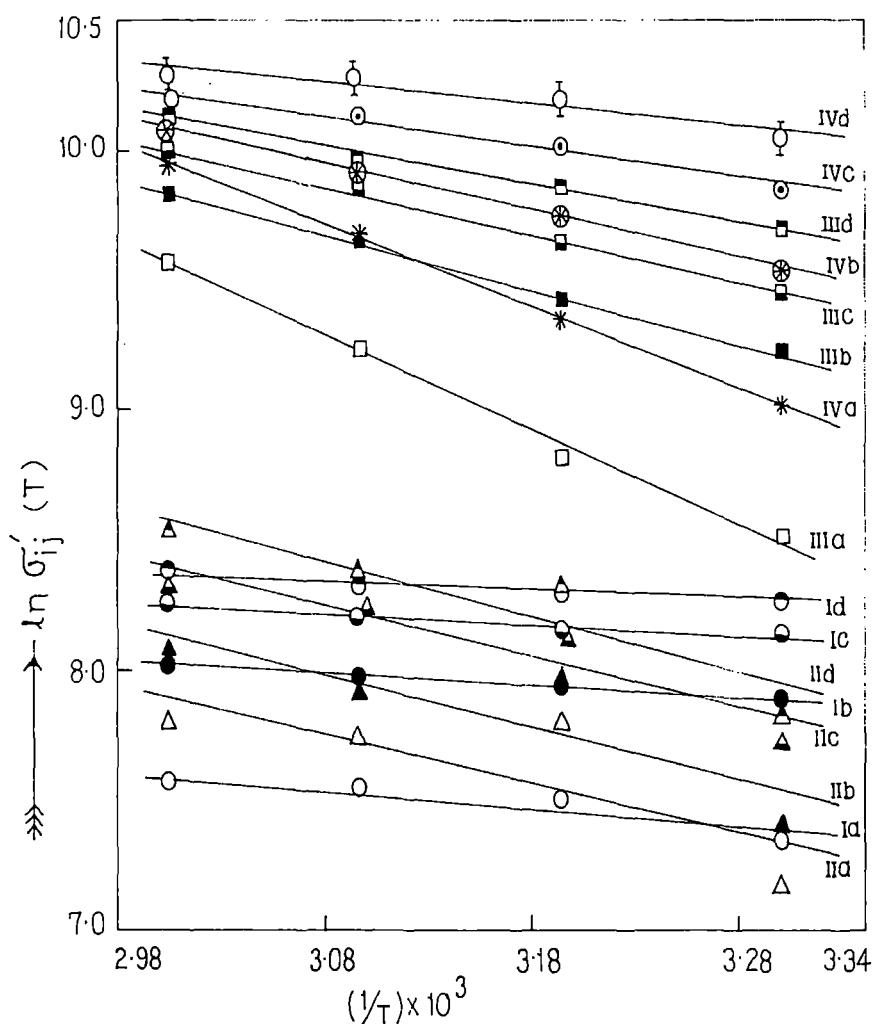


Figure 10.3: Plot of $\ln \sigma'_{ij} (T)$ against $1/T$ of aprotic polar liquids in C_6H_6 and CCl_4 at different weight fractions (w_j) of solute under 500 KHz electric field.

(I) DMF in C_6H_6

(Ia) $w_j = 0.3520$ (—○—), (Ib) $w_j = 0.5218$ (—●—)

(Ic) $w_j = 0.6563$ (—◐—), (Id) $w_j = 0.7500$ (—◑—)

(II) DMF in CCl_4

(IIa) $w_j = 0.3772$ (—△—), (IIb) $w_j = 0.4760$ (—▲—),

(IIc) $w_j = 0.6248$ (—◀—), (IId) $w_j = 0.7316$ (—▶—)

(III) DMSO in C_6H_6

(IIIa) $w_j = 0.1124$ (—□—), (IIIb) $w_j = 0.2021$ (—■—),

(IIIc) $w_j = 0.2754$ (—◻—), (IIId) $w_j = 0.3878$ (—◼—),

(IV) DMSO in CCl_4

(IVa) $w_j = 0.0954$ (—*—), (IVb) $w_j = 0.1742$ (—⊗—),

(IVc) $w_j = 0.2601$ (—○—), (IVd) $w_j = 0.3453$ (—◕—)

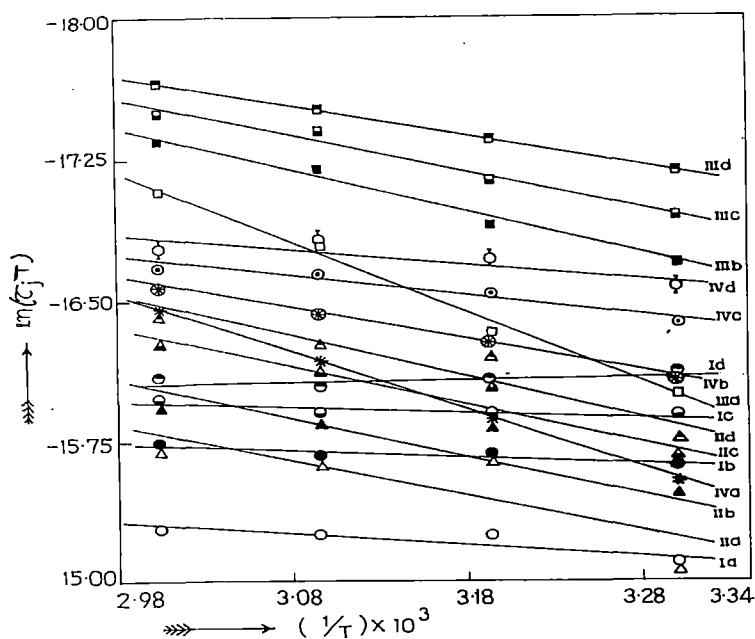


Figure 10.4: Plot of $\ln(\tau_j T)$ against $1/T$ of aprotic polar liquids in C_6H_6 and CCl_4 at different weight fractions (w_j) of solute under 500 KHz electric field.

(I) DMF in C_6H_6

(Ia) $w_j = 0.3520$ (—○—), (Ib) $w_j = 0.5218$ (—●—) (Ic) $w_j = 0.6563$ (—◐—), (Id) $w_j = 0.7500$ (—◑—)

(II) DMF in CCl_4

(IIa) $w_j = 0.3772$ (—△—), (IIb) $w_j = 0.4760$ (—▲—), (IIc) $w_j = 0.6248$ (—◀—), (IId) $w_j = 0.7316$ (—◁—)

(III) DMSO in C_6H_6

(IIIa) $w_j = 0.1124$ (—□—), (IIIb) $w_j = 0.2021$ (—■—), (IIIc) $w_j = 0.2754$ (—◓—), (IIId) $w_j = 0.3878$ (—◔—),

(IV) DMSO in CCl_4 (IVa) $w_j = 0.0954$ (—*—), (IVb) $w_j = 0.1742$ (—⊗—), (IVc) $w_j = 0.2601$ (—⊙—),

(IVd) $w_j = 0.3453$ (—⊚—)

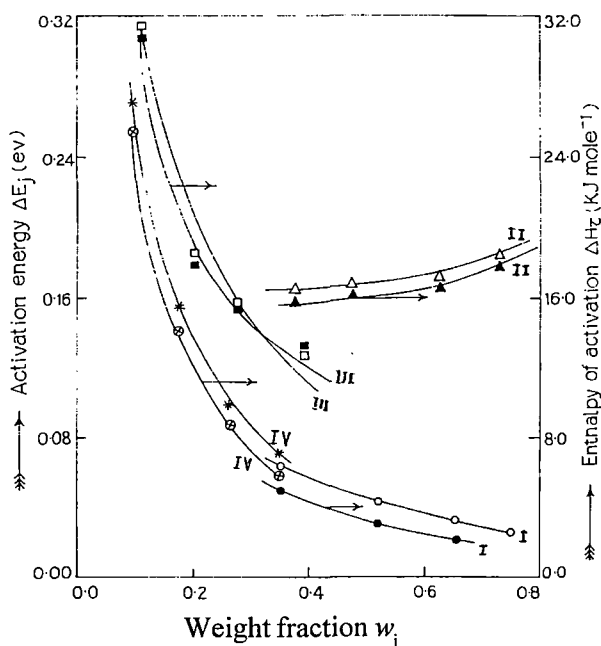


Figure 10.5: Variation of semiconduction activation energy (ΔE_j) and enthalpy of activation due to dielectric relaxation (ΔH_τ) against weight fraction of solute w_j of aprotic polar liquids in benzene and carbon tetrachloride under 500 KHz electric field.

$\Delta E_j - w_j$ variation

(I) DMF in C_6H_6 (—○—),

(II) DMF in CCl_4 (—△—),

(III) DMSO in C_6H_6 (—□—),

(IV) DMSO in CCl_4 (—*—),

$\Delta H_\tau - w_j$ variation

(I) DMF in C_6H_6 (—●—),

(II) DMF in CCl_4 (—▲—),

(III) DMSO in C_6H_6 (—■—),

(IV) DMSO in CCl_4 (—⊗—)

10.3. Results and Discussion

The linear dependence of σ'_{ij} on $1/\eta_{ij}$ is obtained graphically by applying regression analysis on the data. As a result curves of Figure 10.1 with proper symbols of the experimental data are worked out. It is seen in Figure 10.1 that σ'_{ij} shows excellent linear dependence on $1/\eta_{ij}$ for both DMF and DMSO in C_6H_6 and CCl_4 at different experimental temperatures. The slope of the linear equation:

$$\sigma'_{ij} = \left(\frac{\epsilon_{oij} - \epsilon_{\infty ij}}{4\pi} \right) \omega^2 \tau + \left(\frac{ne^2}{6\pi a} \right) \frac{1}{\eta_{ij}} \quad (10.1)$$

of Figure 10.1 are placed in the 4th column of Table 10.2. They were used to obtain 'n' with the knowledge of molecular radius 'a' of the gas kinetic values. The estimated 'n' are shown in the 5th column of Table 10.2 at different experimental temperatures for each system.

Figure 10.1 shows that σ'_{ij} decreases with rise of $1/\eta_{ij}$ having negative slope for all the systems at all temperatures except for DMF in CCl_4 which showed positive slope. This happens probably due to the fact that DMF is less viscous [12,14] than CCl_4 .

The values of 'n' then used to obtain τ_j at different concentrations and temperatures from [7] :

$$\tau_j = \frac{2na^2e^2}{3\sigma'_{ij}k_B T} \quad (10.2)$$

τ_j 's at different temperatures and concentrations w_j 's are entered in Table 10.1. A simple extrapolation technique is, however employed on the measured τ_j 's of Eq (10.2) and the following polynomial equations between τ_j and w_j were worked out. It is evident when $w_j = 0$ one gets τ_j at infinite dilution.

I. DMF in C₆H₆

$$\tau_j \times 10^{10} = 119.48 - 430.95 w_j + 377.71 w_j^2 \text{ at } 30^\circ\text{C}$$

$$\tau_j \times 10^{10} = 74.52 - 275.72 w_j + 248.67 w_j^2 \text{ at } 40^\circ\text{C}$$

$$\tau_j \times 10^{10} = 90.67 - 347.83 w_j + 318.50 w_j^2 \text{ at } 50^\circ\text{C}$$

$$\tau_j \times 10^{10} = 44.08 - 144.54 w_j + 122.71 w_j^2 \text{ at } 60^\circ\text{C}$$

II. DMF in CCl₄

$$\tau_j \times 10^{10} = 37.59 - 97.26 w_j + 69.63 w_j^2 \text{ at } 30^\circ\text{C}$$

$$\tau_j \times 10^{10} = 10.62 - 18.56 w_j + 10.89 w_j^2 \text{ at } 40^\circ\text{C}$$

$$\tau_j \times 10^{10} = 15.92 - 36.78 w_j + 24.89 w_j^2 \text{ at } 50^\circ\text{C}$$

$$\tau_j \times 10^{10} = 15.10 - 35.87 w_j + 24.28 w_j^2 \text{ at } 60^\circ\text{C}$$

III. DMSO in C₆H₆

$$\tau_j \times 10^{10} = 22.68 - 153.63 w_j + 242.52 w_j^2 \text{ at } 30^\circ\text{C}$$

$$\tau_j \times 10^{10} = 5.99 - 31.36 w_j + 45.44 w_j^2 \text{ at } 40^\circ\text{C}$$

$$\tau_j \times 10^{10} = 2.94 - 12.86 w_{jj} + 17.82 w_j^2 \text{ at } 50^\circ\text{C}$$

$$\tau_j \times 10^{10} = 1.62 - 4.78 w_{jj} + 5.68 w_j^2 \text{ at } 60^\circ\text{C}$$

IV. DMSO in CCl₄

$$\tau_j \times 10^{10} = 11.37 - 63.92 w_j + 100.12 w_j^2 \text{ at } 30^\circ\text{C}$$

$$\tau_j \times 10^{10} = 6.68 - 31.12 w_j + 49.81 w_j^2 \text{ at } 40^\circ\text{C}$$

$$\tau_j \times 10^{10} = 4.21 - 14.93 w_j + 21.20 w_j^2 \text{ at } 50^\circ\text{C}$$

$$\tau_j \times 10^{10} = 2.49 - 4.16 w_j + 4.32 w_j^2 \text{ at } 60^\circ\text{C}.$$

τ_j 's so estimated are presented in the 6th column of Table 10.2. They are supposed to be free from polar-polar interaction [11,18].

According to Smyth [8] real part σ'_{ij} of complex hf σ_{ij}^* is written as

$$\sigma'_{ij} = \frac{4\pi^2 f^2 N \tau_j d_i \mu_j^2 (\epsilon_{oij} + 2) (n_{Dij}^2 + 2)}{27 M_j k_B T} w_j \quad (10.3)$$

Eq. (10.3) on differentiation w.r. to w_j and at $w_j \rightarrow 0$ yields

$$\mu_j = \left[\frac{27 M_j k_B T \beta}{4\pi^2 f^2 N \tau_j d_i (\epsilon_{oi} + 2) (n_{Di}^2 + 2)} \right]^{1/2} \quad (10.4)$$

where

- M_j = molecular weight of solute
- f = frequency of applied electric field
- k_B = Boltzmann constant = 1.38×10^{-16} erg mole⁻¹ K⁻¹
- N = Avogadro's number = 6.023×10^{23}
- d_i = density of solvent
- ϵ_{oi} = static relative permittivity of solvent
- n_{Di} = refractive index of solvent.

The linear coefficient $\beta = (d\sigma'_{ij}/dw_j)_{w_j \rightarrow 0}$ of $\sigma'_{ij} - w_j$ curves of $\sigma'_{ij} = \alpha + \beta w_j + \gamma w_j^2$ as seen in the 8th column of Table 10.2 was used to estimate μ_j from Eq. (10.4).

The μ_{theo} 's obtained by vector addition of group moments [9] of planer molecules are placed in 11th column together with the estimated μ_j 's in the 10th column of Table 10.2. It is seen that for DMF μ_j 's $< \mu_{\text{theo}}$'s probably due to

the fact that under rf electric field the greater inter ionic forces hinders the dipolar rotation [12] for lower μ_j 's. But for DMSO inter ionic forces are weaker giving μ_j 's $>$ μ_{theo} 's.

μ_j 's are plotted against $t^\circ\text{C}$ in Figure 10.2. The variation of μ_j 's with respect to t in $^\circ\text{C}$ are, however, represented by the following equations :

I. DMF in C_6H_6

$$\mu_j = 0.988 - 0.0239 t + 0.0005t^2$$

II. DMF in CCl_4

$$\mu_j = -2.622 + 0.1566t - 0.0015t^2$$

III. DMSO in C_6H_6

$$\mu_j = -15.5795 + 0.8343t - 0.0041t^2$$

IV. DMSO in CCl_4

$$\mu_j = -7.773 + 0.6649t - 0.0061t^2$$

Curve I for DMF in C_6H_6 showed monotonic increase of μ_j with $t^\circ\text{C}$ for its increasing molecular asymmetry attained at higher temperature. Other curves on the other hand are convex in nature showing $\mu_j = 0$ both at lower and higher temperatures due to symmetry [11] gained by the molecules. The above nature of $\mu_j - t$ curves are interpreted by the rupture of monomer and dimer formations due to stretching of bond moments of flexible polar groups attached to molecules by thermal agitation.

The ionic conduction due to mobility of free charges in an insulating dipolar liquid occurs for ϵ'' . Rf $\sigma'_{ij}(T)$ can be expressed by [19,20]:

$$\sigma'_{ij}(T) = \sigma'_i \exp(-\Delta E_j/k_B T) \quad (10.5)$$

$$\ln \sigma'_{ij}(T) = \ln \sigma'_i - \left(\frac{\Delta E_j}{k_B}\right) \cdot \frac{1}{T} \quad (10.6)$$

Table 10.1 : Radio frequency conductivity (σ'_{ij}), reciprocal of solution viscosity ($1/\eta_{ij}$) and estimated relaxation times (τ_j) of aprotic polar liquids in benzene (C_6H_6) and carbontetrachloride (CCl_4) at different concentrations (w_j) and temperatures under 500 KHz electric field.

Systems with serial number & Molecular weight (M_j)	Weight fraction w_j of solute	Rf conductivity $\sigma'_{ij} \times 10^{-3}$ in $\Omega^{-1} \text{ cm}^{-1}$				Reciprocal of solution viscosity $1/\eta_{ij} \times 10^{-3}$ in poise ⁻¹				Estimated Relaxation times $\tau_j \times 10^{10}$ sec.			
		30°C	40°C	50°C	60°C	30°C	40°C	50°C	60°C	30°C	40°C	50°C	60°C
(I) DMF in C_6H_6 $M_j=73$ gm.	0.0984	0.1620	0.2400	0.2000	0.4069	0.2315	0.1985	0.1739	0.2743	88.18	57.05	69.67	32.86
	0.2143	0.4064	0.9000	0.9800	0.8159	0.2265	0.1936	0.1690	0.2694	35.15	15.21	14.22	16.39
	0.3520	1.5400	1.8000	1.9000	1.9203	0.2208	0.1881	0.1635	0.2637	9.28	7.61	7.33	6.96
	0.5218	2.6400	2.8000	2.9000	3.0761	0.2141	0.1818	0.1572	0.2570	5.41	4.89	4.80	4.35
	0.6563	3.4600	3.4200	3.6200	3.8630	0.2091	0.1770	0.1526	0.2520	4.13	4.00	3.85	3.46
	0.7105	3.7600	3.8200	4.0000	4.1221	0.2071	0.1752	0.1508	0.2500	3.79	3.58	3.48	3.24
	0.7500	3.9800	3.0400	4.1200	4.3547	0.2058	0.1739	0.1495	0.2486	3.34	3.39	3.38	3.07
(II) DMF in CCl_4 $M_j=73$ gm.	0.1315	0.4186	1.4100	0.9446	0.9600	0.1176	0.1360	0.1593	0.1901	28.98	8.56	12.25	11.47
	0.2324	0.8094	1.8000	1.4626	1.5000	0.1199	0.1389	0.1630	0.1948	14.99	6.71	7.91	7.34
	0.3772	1.2900	2.4300	2.3100	2.4300	0.1236	0.1433	0.1685	0.2019	9.40	4.97	5.01	4.53
	0.4760	1.6500	2.8500	2.8500	3.1200	0.1261	0.1465	0.1725	0.2071	7.35	4.24	4.06	3.53
	0.5478	1.9500	3.1800	3.2100	3.6900	0.1281	0.1489	0.1755	0.2111	6.22	3.80	3.61	2.98
	0.6248	2.2500	3.5100	3.7500	4.2300	0.1303	0.1551	0.1789	0.2155	5.39	3.44	3.09	2.60
	0.7316	2.5766	4.0539	4.3296	5.0659	0.1334	0.1554	0.1838	0.2219	4.71	2.98	2.67	2.16
0.8583	3.0927	4.7072	5.1506	6.1785	0.1373	0.1602	0.1899	0.2301	3.92	2.57	2.25	1.78	

Contd...

Systems with serial number & Molecular weight (M_j)	Weight fraction w_i of solute	Rf conductivity $\sigma'_{ij} \times 10^{-3}$ in $\Omega^{-1} \text{ cm}^{-1}$				Reciprocal of solution viscosity $1/\eta_{ij} \times 10^{-3}$ in poise^{-1}				Estimated Relaxation times $\tau_j \times 10^{10}$ sec.			
		30°C	40°C	50°C	60°C	30°C	40°C	50°C	60°C	30°C	40°C	50°C	60°C
(III) DMSO in C_6H_6 $M_j = 78\text{gm}$	0.0596	1.0020	3.7500	6.8003	12.0001	0.1505	0.1763	0.2122	0.2626	18.39	4.71	2.40	1.39
	0.1124	5.0064	6.7504	10.4001	14.600	0.1322	0.1579	0.1949	0.2498	3.67	2.62	1.57	1.14
	0.1597	7.8003	9.7506	13.4020	16.9021	0.1192	0.1444	0.1815	0.2394	2.36	1.81	1.22	0.98
	0.2021	10.1095	12.1500	15.6000	18.9000	0.1096	0.1342	0.1711	0.2307	1.82	1.46	1.05	0.88
	0.2754	12.8031	15.4500	19.0002	21.8906	0.0962	0.1195	0.1555	0.2172	1.44	1.14	0.86	0.76
	0.3878	16.2001	19.2001	21.2000	25.6003	0.0810	0.1023	0.1366	0.1992	1.14	0.92	0.77	0.65
	0.4516	17.6000	21.1500	25.1000	27.6000	0.0743	0.0946	0.1277	0.1903	1.05	0.84	0.65	0.60
(IV) DMSO in CCl_4 $M_j = 78\text{gm}$	0.0657	5.8200	9.3001	13.6000	19.9600	0.1035	0.1219	0.1463	0.1802	8.28	5.07	3.40	2.25
	0.0954	8.2436	11.7000	15.7010	21.1601	0.0991	0.1177	0.1427	0.1784	5.84	4.03	2.94	2.13
	0.1233	10.3700	13.9021	17.5012	22.1200	0.0954	0.1140	0.1395	0.1768	4.65	3.40	2.64	2.03
	0.1742	13.9450	17.5003	20.7004	23.8003	0.0892	0.1078	0.1341	0.1739	3.46	2.70	2.23	1.89
	0.2195	17.0024	20.2011	23.1509	25.2400	0.0843	0.1029	0.1296	0.1714	2.83	2.34	1.99	1.78
	0.2601	18.9500	22.6000	25.6000	26.4407	0.0804	0.0988	0.1258	0.1692	2.54	2.09	1.80	1.70
	0.2967	20.7720	24.6004	27.5005	27.6400	0.0772	0.0954	0.1225	0.1673	2.32	1.92	1.68	1.68
	0.3453	23.0450	27.1000	29.8000	29.0800	0.0732	0.0912	0.1185	0.1648	2.09	1.74	1.55	1.55

Table 10.2 : Intercept and slope of fitted linear curves of Figure 10.1, number density of free ions (n), relaxation time τ_j at $w_j=0$, coefficients α , β , γ , of $\sigma_{ij} - w_j$ fitted equations together with estimated and theoretical dipole moments μ 's of aprotic polar liquids in C_6H_6 and CCl_4 at different temperatures under 500 KHz electric field.

Systems with serial number and molecular weight	Temperature in $^{\circ}C$	Intercept & slope of $\sigma_{ij} \times 10^{-3}$ vs. $(1/\eta_{ij}) \times 10^{-3}$ fitted curves of Fig.10.1		Number density of free ions $n \times 10^{-14}$ per c.c.	Relaxation time $\tau_j \times 10^{10}$ sec. at $w_j = 0$	Coefficients α, β, γ , of the fitted equation $\sigma'_{ij} = \alpha + \beta w_j + \gamma w_j^2$			Estimated dipole moment μ_j in Debye	Theoretical dipole moment in μ_{theo} in Debye
		intercept (A)	slope $B \times 10^{-3}$			$\alpha \times 10^{-3}$	$\beta \times 10^{-3}$	$\gamma \times 10^{-3}$		
(i) DMF in benzene $M_j = 73$ gm	30	35.9890	-0.1558	3.9774	119.48	-0.5278	5.4103	0.9083	0.63	3.82
	40	30.8290	-0.1543	3.9384	74.52	-0.4028	6.4416	-0.7380	0.89	
	50	28.3775	-0.1620	4.1355	90.67	-0.5082	7.3149	-1.4802	0.78	
	60	44.2220	-0.1603	4.0917	44.08	-0.3509	6.4678	-0.1793	1.22	
(ii) DMF in carbon tetrachloride $M_j = 73$ gm	30	-15.0763	0.1323	3.3772	37.59	-0.0043	3.5322	0.1259	0.69	3.82
	40	-17.0963	0.1361	3.4734	10.62	0.9225	3.5938	0.9405	1.35	
	50	-20.4090	0.1346	3.4350	15.92	0.2598	5.0935	0.6902	135	
	60	-24.1995	0.1320	3.3692	15.10	0.2471	4.9702	2.2676	1.41	
(iii) DMSO in benzene $M_j = 78$ gm.	30	33.8410	-0.2180	5.4128	22.68	-3.2997	80.9619	-77.7434	5.80	4.55
	40	41.3407	-0.2165	5.3747	5.99	-0.5318	73.3962	-56.7150	11.01	
	50	50.6499	-0.2061	5.1153	2.94	2.9616	72.5886	-56.3693	16.01	
	60	68.8253	-0.2166	5.3779	1.62	8.6837	57.0748	-33.9152	19.57	
(iv) DMSO in carbon tetrachloride $M_j = 78$ gm.	30	64.9110	-0.5719	14.1790	11.37	-0.0014	94.2025	-80.0827	6.72	4.55
	40	79.7491	-0.5779	14.3473	6.68	3.8179	88.6445	-62.0821	8.74	
	50	98.9472	-0.5836	14.4872	4.21	8.9490	74.0356	-39.3454	10.34	
	60	125.6921	-0.5862	14.5513	2.49	17.6255	37.6434	-13.2139	9.90	

Table 10.3 : Intercepts and slopes of $\ln \sigma'_{ij}(T) - 1/T$ fitted linear curves of Figure 10.3, activation energies (ΔE_j), Debye and Kalman factors of dipolar aprotic polar liquids in benzene under 500 KHz electric field at different concentrations.

Systems with serial number	Weight fraction of solute (w_j)	Temperature in Kelvin (T)	R.f. conductivity $\sigma'_{ij} \times 10^{-3}$ in $\Omega^{-1} \text{ cm}^{-1}$	Intercept & slope of $\ln \sigma'_{ij}(T)$ vs. $1/T$ fitted equation		Activation energy ΔE_j of solute in eV	Debye factor $(\tau_j T/\eta) \times 10^6$	Kalman factor $(\tau_j T/\eta^2) \times 10^8$
				Intercept (C)	Slope $m \times 10^{-3}$			
(I) DMF in benzene (C_6H_6)	0.3520	303	1.5400	9.7897	-0.7316	0.0631	50.1003	197.9447
		313	1.8000				48.3058	176.0617
		323	1.9000				55.8926	185.3988
		333	1.9203				64.6249	193.2359
	0.5218	303	2.6400	9.5227	-0.4979	0.0429	29.2252	56.8518
		313	2.8000				31.0523	54.7470
		323	2.9000				36.6164	57.5515
		333	3.0761				40.3453	55.8763
	0.6563	303	3.4600	9.3993	-0.3857	0.0332	22.3010	31.1670
		313	3.4200				25.4261	31.9406
		323	3.6200				29.3373	32.5396
		333	3.8630				32.1222	31.0626
0.7500	303	3.9800	9.2352	-0.2894	0.0249	18.0558	8.6841	
	313	3.0400				21.5207	9.0592	
	323	4.1200				25.7778	9.2876	
	333	4.3547				28.5025	8.6517	

Contd...

Systems with serial number	Weight fraction of solute (w_j)	Temperature in Kelvin (T)	R.f. conductivity $\sigma'_{ij} \times 10^{-3}$ in $\Omega^{-1} \text{ cm}^{-1}$	Intercept & slope of $\ln \sigma'_{ij} (T)$ vs. $1/T$ fitted equation		Activation energy ΔE_j of solute in eV	Debye factor $(\tau_j T / \eta) \times 10^6$	Kalman factor $(\tau_j T / \eta^2) \times 10^8$
				Intercept (C)	Slope $m \times 10^{-3}$			
(II) DMF in Carbon tetrachloride (CCl_4)	0.3772	303	1.2900	13.6151	-0.1903	0.1640	32.6481	6570.2763
		313	2.4300				20.5863	4231.8254
		323	2.3100				25.0546	5270.9757
		333	2.4300				27.8021	6001.1005
	0.4760	303	1.6500	14.0027	-0.1957	0.1687	25.5234	6394.3492
		313	2.8500				17.5502	4521.1758
		323	2.8500				20.3088	5393.3334
		333	3.1200				21.6539	5947.7380
	0.6248	303	2.2500	14.4049	-0.1998	0.1722	18.7181	5633.8900
		313	3.5100				14.2531	4435.9495
		323	3.7500				15.4329	4981.5824
		333	4.2300				15.9720	5368.4248
0.7316	303	2.5766	15.0325	-0.2149	0.1852	16.3432	7798.8866	
	313	4.0539				12.3394	6174.4696	
	323	4.3296				13.3675	7044.0690	
	333	5.0959				13.2599	7399.9411	

Contd...

Systems with serial number	Weight fraction of solute (w_j)	Temperature in Kelvin (T)	R.f. conductivity $\sigma'_{ij} \times 10^{-3}$ in $\Omega^{-1} \text{cm}^{-1}$	Intercept & slope of $\ln \sigma'_{ij}(T)$ vs. $1/T$ fitted equation		Activation energy ΔE_j of solute in eV	Debye factor $(\tau_j T/\eta) \times 10^6$	Kalman factor $(\tau_j T/\eta^2) \times 10^8$
				Intercept (C)	Slope $m \times 10^{-3}$			
(III) DMSO in benzene (C_6H_6)	0.1124	303	5.0064	20.6028	- 3.6714	0.3164	19.8435	High value
		313	6.7504				16.6311	
		323	10.4001				11.9514	
		333	14.6000				10.5713	
	0.2021	303	10.1094	16.2840	- 2.1445	0.1848	9.8245	10827.861
		313	12.1500				9.2395	10811.879
		323	15.6000				7.9651	9996.0246
		333	18.9000				9.1674	11071.221
	0.2754	303	12.8031	15.5148	- 1.8350	0.1582	7.7613	2846.2402
		313	15.4500				7.2646	2751.927
		323	19.0002				6.5397	2572.9898
		333	21.8906				7.0537	2893.4703
0.3878	303	16.2001	14.5869	- 1.4833	0.1278	6.1302	706.9345	
	313	19.2001				5.8485	676.8529	
	323	21.2000				5.8614	681.1654	
	333	25.6003				6.0235	703.2188	

Contd...

Systems with serial number	Weight fraction of solute (w_j)	Temperature in Kelvin (T)	R.f. conductivity $\sigma'_{ij} \times 10^{-3}$ in $\Omega^{-1} \text{ cm}^{-1}$	Intercept & slope of $\ln \sigma'_{ij} (T)$ vs. $1/T$ fitted equation		Activation energy ΔE_j of solute in eV	Debye factor $(\tau_j T / \eta) \times 10^6$	Kalman factor $(\tau_j T / \eta^2) \times 10^8$
				Intercept (C)	Slope $m \times 10^{-3}$			
(IV) DMSO in carbon tetrachloride (CCl_4)	0.0954	303	8.2436	19.4253	- 3.1519	0.2717	20.2944	153513.13
		313	11.7000				16.7094	144138.42
		323	15.7010				14.7127	146457.23
		333	21.1601				13.0451	152207.23
	0.1742	303	13.9450	15.4750	- 1.7923	0.1545	11.9961	1581.5724
		313	17.5003				11.1713	1485.2464
		323	20.7004				11.1571	1496.9883
		333	23.8003				11.5970	1571.8872
	0.2601	303	18.9500	13.6495	- 1.1426	0.0985	8.8296	164.3480
		313	22.6000				8.6488	152.9701
		323	25.6000				9.0217	150.9270
		333	26.4407				10.4434	164.2551
0.3453	303	23.0450	12.7630	- 0.8114	0.0699	7.2602	49.7633	
	313	27.1000				7.2156	45.5918	
	323	29.8000				7.7514	44.8189	
	333	29.0800				9.4924	49.7418	

Contd...

Table 10.4 : Intercepts and slopes of fitted linear curves of Figure 10.4, enthalpy of activation ΔH_{τ} in KJ mole⁻¹, entropy of activation ΔS_{τ} in J mole⁻¹ K⁻¹, free energy of activation ΔF_{τ} in KJ mole⁻¹, dimensionless parameter $\gamma (= \Delta H_{\tau} / \Delta H_{\eta})$ of dipolar aprotic polar liquids in benzene and carbon tetrachloride at different concentrations under 500 KHz electric field.

Systems with Serial number	Weight fraction of solute (w_j)	Temperature in Kelvin	Intercept & slope of $\ln(\tau_j T)$ vs. $(1/T)$ fitted equation		Enthalpy of activation ΔH_{τ} in KJ mole ⁻¹	$\gamma = \frac{\Delta H_{\tau}}{\Delta H_{\eta}}$	Enthalpy of activation ΔH_{η} in KJ mole ⁻¹ due to viscous flow	Entropy of activation ΔS_{τ} in J mole ⁻¹ K ⁻¹	Free energy of activation ΔF_{τ} in KJ mole ⁻¹
			Intercept (c)	Slope $m \times 10^{-3}$					
(I) DMF in benzene (C_6H_6)	0.3520	303						- 55.7322	21.8449
		313	- 17.0955	0.5966	4.9580	0.3766	13.1326	- 54.8765	22.1343
		323						- 55.3234	22.8274
		333						- 55.6075	23.4753
	0.5218	303						- 57.6571	20.4877
		313	- 16.8291	0.3631	3.0176	0.2399	12.5785	- 57.4038	20.9850
		323						- 57.8162	21.6922
		333						- 57.5194	22.1716
	0.6563	303						- 58.4739	19.8068*
		313	- 16.7073	0.2514	2.0892	0.1761	11.8637	- 58.7086	20.4650
		323						- 58.8485	21.0973
		333						- 58.4131	21.5408
	0.7500	303						- 65.4166	19.2752
		313	- 15.8656	0.0066	- 0.5460	- 0.0297	18.3540	- 65.7424	20.0314
		323						- 65.9326	20.7502
		333						- 65.3336	21.2101

Contd...

Systems with Serial number	Weight fraction of solute (w_j)	Temperature in Kelvin	Intercept & slope of $\ln(\tau_j T)$ vs. $(1/T)$ fitted equation		Enthalpy of activation ΔH_τ in KJ mole ⁻¹	$\gamma = \frac{\Delta H_\tau}{\Delta H_\eta}$	Enthalpy of activation ΔH_η in KJ mole ⁻¹ due to viscous flow	Entropy of activation ΔS_τ in J mole ⁻¹ K ⁻¹	Free energy of activation ΔF_τ in KJ mole ⁻¹
			Intercept (c)	Slope $m \times 10^{-3}$					
(II) DMF in Carbon tetrachloride CCl_4	0.3772	303						-19.5998	21.8790
		313						-16.2519	21.0271
		323	-21.5622	1.9182	15.9403	1.1475	13.8912	-18.1566	21.8049
		333						-19.0568	22.2862
	0.4760	303						-16.0755	21.2593
		313	-21.9484	1.9721	16.3884	1.1937	13.7290	-13.4947	20.6122
		323						-15.0245	21.2413
		333						-15.6347	21.5947
	0.6248	303						-12.3714	20.4784
		313	-22.3520	2.0132	16.7299	1.2324	13.5750	-10.6743	20.0710
		323						-11.6856	20.5044
		333						-12.0799	20.7525
	0.7316	303						-7.1320	20.1368
		313	-22.9765	2.1631	17.9758	1.3296	13.5197	-5.4958	19.6960
		323						-6.6344	20.1187
		333						-6.7921	20.2376

Contd...

Systems with Serial number	Weight fraction of solute (w_1)	Temperature in Kelvin	Intercept & slope of $\ln(\tau_1 T)$ vs. $(1/T)$ fitted equation		Enthalpy of activation ΔH_τ in KJ mole ⁻¹	$\gamma = \frac{\Delta H_\tau}{\Delta H_\eta}$	Enthalpy of activation ΔH_η in KJ mole ⁻¹ due to viscous flow	Entropy of activation ΔS_τ in J mole ⁻¹ K ⁻¹	Free energy of activation ΔF_τ in KJ mole ⁻¹
			Intercept (c)	Slope $m \times 10^{-3}$					
		303						38.2853	19.5129
		313						37.5476	19.3609
	0.1124	323	- 28.3417	3.7441	31.1133	2.4796	12.5477	38.4717	18.6869
		333						37.9820	18.4653
	0.2021	303						1.2812	17.7428
		313	- 23.9116	2.1818	18.1310	1.4630	12.3932	0.9551	17.8321
		323						1.6509	17.5978
		333						1.1399	17.7514
(III) DMSO in benzene (C_6H_6)	0.2754	303						- 4.3130	17.1493
		313	- 23.2495	1.9064	15.8424	1.2507	12.6665	- 4.3584	17.2066
		323						- 3.7961	17.0685
		333						- 4.5145	17.3457
	0.3878	303						- 11.9094	16.5553
		313	- 22.3323	1.5579	12.9467	1.0275	12.6007	- 11.8082	16.6427
		323						- 11.8513	16.7747
		333						- 11.8985	16.9089

Contd...

Systems with Serial number	Weight fraction of solute (w_j)	Temperature in Kelvin	Intercept & slope of $\ln(\tau_j T)$ vs. $(1/T)$ fitted equation		Enthalpy of activation ΔH_τ in KJ mole ⁻¹	$\gamma = \frac{\Delta H_\tau}{\Delta H_\eta}$	Enthalpy of activation ΔH_η in KJ mole ⁻¹ due to viscous flow	Entropy of activation ΔS_τ in J mole ⁻¹ K ⁻¹	Free energy of activation ΔF_τ in KJ mole ⁻¹
			Intercept (c)	Slope $m \times 10^{-3}$					
		303						15.7630	20.6820
	0.0954	313	-25.6616	3.0636	25.4582	1.9124	13.3122	15.8904	20.4845
		323						15.7341	20.7361
		333						15.8134	20.1924
		303						-17.1520	19.3582
	0.1742	313	-21.7120	1.7041	14.1611	1.0583	13.3810	-16.8568	19.4373
		323						-16.9425	19.6335
		333						-17.1341	19.8667
(IV) DMSO in Carbon tetra chloride (CCl ₄)	0.2601	303						-32.4419	18.5865
		313	-19.8843	1.0537	8.7566	0.6454	13.5677	-31.9969	18.7716
		323						-31.9094	19.0633
		333						-32.4933	19.5769
		303						-39.8743	18.0937
	0.3453	313	-19.0003	0.7234	6.0118	0.4347	13.8298	-39.2606	18.3004
		323						-39.1461	18.6560
		333						-39.9423	19.3126

Which shows that $\ln \sigma'_{ij}(T)$ is a linear function of $1/T$ as displayed in Figure 10.3. The experimental points were found to satisfy the curves of Figure 10.3. σ'_1 is the pre exponential factor which is constant for a given liquid mixture. The slope of the linear curves of Figure 10.3 as seen in the 6th column of Table 10.3 were utilised to get ΔE_j in order to place them in the 7th column of the same table at different concentrations w_j 's. Non linear variation of ΔE_j with w_j of Figure 10.5 shows probable existence of solute-solvent molecular associations [12].

The rotating dipoles under rf electric field requires an free energy of activation ΔF_τ to overcome the potential energy barrier between two equilibrium positions. ΔF_τ is, however, related to measured τ_j by [10].

$$\tau_j = A/T \exp(\Delta F_\tau/RT) \quad (10.7)$$

$$\text{where } \Delta F_\tau = \Delta H_\tau - T \Delta S_\tau \quad (10.8)$$

$$\text{or } \ln(\tau_j T) = \ln A' + \left(\frac{\Delta H_\tau}{R}\right) \cdot \frac{1}{T} \quad (10.9)$$

$$\text{where } A' = A e^{-\Delta S_\tau/R} \text{ and } A = h/k_B$$

The intercepts and slopes of Eq (10.9) as shown graphically in Figure 10.4 were accurately estimated in order to place them in 4th and 5th columns of Table 10.4. They were used to compute the thermodynamic energy parameters ΔH_τ , ΔS_τ and ΔF_τ (Table 10.4) due to dielectric relaxation. The variation of ΔH_τ with w_j of Figure 10.5 are non linear except for DMF in C_6H_6 probably due to solute-solvent molecular associations [12]. The 9th column of Table 10.4 showed positive ΔS_τ for DMSO in C_6H_6 (System III) at $w_j = 0.1124$ and 0.2021 and for DMSO in CCl_4 (System IV) at $w_j = 0.0954$. This fact suggests that configuration involved in dipolar association has an activated state which is less ordered than the normal state [12,16]. For system III and IV ΔS_τ passes over from positive to negative values beyond a certain concentration suggesting the fact that the systems becomes more ordered with increase in w_j 's due to solute-solvent and

solute-solute molecular association. This fact is also confirmed by the sharp fall of both ΔE_j and ΔH_τ with w_j as found in Figure 10.5. The enthalpy of activation due to viscous flow was obtained from the slope of the linear equation of $\ln(\tau_j T)$ against $\ln \eta$ at different concentrations for each system. It is evident from the 7th column of Table 10.4 that $\gamma = (\Delta H_\tau / \Delta H_\eta) > 0.50$ for all the systems except DMF in C_6H_6 showing solvent environment around the solute molecule. It behaves as solid phase rotators [11]. The non associative behaviour of DMF in C_6H_6 is, however, confirmed by the linear variation of both ΔE_j and ΔH_τ with w_j as displayed in Figure 10.5. The -Ve value of γ and ΔH_τ for DMF in C_6H_6 at $w_j = 0.7500$ arises probably due to experimental uncertainty. The Debye ($\tau_j T / \eta$) and Kalman ($\tau_j T / \eta^\gamma$) factors in 8th and 9th columns of Table 10.4 showed almost the constant value at all concentrations for each system. It, therefore, indicates the applicability of Debye — Smyth model [8,21] of dielectric relaxation for aprotic polar liquids too.

10.4. Conclusions

The accurate experimental τ_j 's can be estimated in the limit $w_j = 0$ from the best fitted polynomial equations between the measured τ 's at different weight fractions w_j 's. The reliability of the method is due to the fact that the polar-polar interactions [11,18] are fully avoided. The comparison of the measured rf μ_j 's in terms of τ_j 's at $w_j = 0$ with the theoretical μ_{theo} 's provides a better insight into the structural aspect of dipolar molecules. The role of short range ionic forces in the measured μ_j 's is thus be studied. The nature of μ_j -t curves as seen in the figures establishes the breaking of the dimer into monomer due to thermal agitation [11]. This type of molecular association is further confirmed by non-linear variation of relaxation parameter ΔE_j and ΔH_τ with w_j 's. The curves of $\sigma'_{ij} - 1/\eta_{ij}$, $\ln \sigma'_{ij}(T) - 1/T$ and $\ln(\tau_j T) - 1/T$ are, however, satisfied by the experimental points for aprotic polar liquids to show the validity of the formulation so far derived. The almost constant values of Debye and Kalman factor $\tau_j T / \eta$ and $\tau_j T / \eta^\gamma$ reflects the applicability of Debye-Smyth model of dielectric relaxation on such polar liquid molecules.

References

- [1] F.J. Murphy and S O Morgan, *Bell Syst. Tech J* **18** (1939) 502.
- [2] P Standhammer and W F Seyer, *J Appl. Phys.* **28** (1957) 405.
- [3] I. Adamczewski and B Jachym, *Acta Phys Polon (Poland)* **34** (1968) 1015.
- [4] H V Loheneysen and H Nageral, *J Phys D : Appl Phys (UK)* **4** (1971) 1718.
- [5] S N Sen and R Ghosh, *Indian J Pure & Appl. Phys.* **10** (1972) 701.
- [6] S N Sen and R Ghosh, *J Phys Soc Japan* **33** (1972) 838.
- [7] R Ghosh and Ira Chaudhury, *Indian J Pure & Appl. Phys.* **18** (1980) 669.
- [8] C P Smyth '*Dielectric Behaviour and Structure*' (New York : McGraw Hill 1955).
- [9] S K Sit, N Ghosh, U Saha and S Acharyya *Indian J Phys.* **71B** (1997) 533.
- [10] H Eyring, S Glasstone and K J Laidler '*The Theory of Rate Process*' (New York : McGraw Hill 1941).
- [11] N Ghosh, R C Basak, S K Sit and S Acharyya *J Mol Liquids (Germany)* **85** (2000) 375.
- [12] N Ghosh, R Ghosh, R C Basak, K. Dutta and S Acharyya *Pramana J. Phys.* Communicated 2002.
- [13] A K Ghosh and S N Sen, *J Phys Soc Japan* **48** (1980) 1219.
- [14] R Ghosh and Ira Chaudhury. *Indian J Pure & Appl Phys* **20** (1982) 717.
- [15] R Ghosh and A K Chatterjee. *Indian J Pure & Appl. Phys.* **29** (1991) 650.

- [16] U Saha and R Ghosh *J Phys D : Appl Phys (UK)* **32** (1999) 820.
- [17] '*Hand Book of Chemistry and Physics*' CRC Press 58th Edition 1977-78.
- [18] N Ghosh, A Karmakar, S K Sit and S Acharyya, *Indian J Pure & Appl. Phys* **38** (2000) 574.
- [19] R Ghosh and Ira Chaudhury, *Pramana J Phys* **18** (1981) 319.
- [20] Manisha Gupta and J P Shukla, *Indian J Pure & Appl Phys* **31** (1993) 786.
- [21] P Debye '*Polar Molecules*' (Chemical catalogue) 1929.